CHAPTER 6

6.1 Introduction

The augmented applications of heavy metals and their unrestrained discharge ensued in an increased flux of metallic substances in various environmental segments. The presence of such metals in aqueous streams arising from the discharge of untreated metal containing effluent into water bodies contaminates it and interferes with numerous beneficial usages of water [Sharma et al., 2009]. Heavy metals being recalcitrant and persistent in nature can be harmful to humans, animals, plants and ecosystems [Maksin et al., 2012]. Thus, heavy metal contamination is one of the most important environmental issues posing a serious threat to the environment and biota [Pamukoglu et al., 2006; Sawalha et al., 2007]. Therefore, it is imperative to prevent their passage into aqueous streams by treating industrial effluents prior to their discharge and strictly holding to the regulations.

Ni(II) is discharged mainly from industries including metal finishing and forging, electroplating, batteries manufacturing [Zafar et al., 2009; Yu et al., 1999; Zhao et al., 1999] and known to cause life-threatening complications such as damage to lungs and kidneys, gastrointestinal distress, e.g., nausea, vomiting, diarrhoea, pulmonary fibrosis, renal oedema, and skin dermatitis upon ingestion [Akhtar et al., 2004; Meena et al., 2005].

In past years, several attempts have been made for the removal of heavy metals from wastewater on different materials through adsorption [Apiratikul and Pavasant, 2008; Ngah and Hanafiah, 2008; Kabbashi et al., 2009; Jusoh et al., 2007; Srivastava et al., 2011; Wang, 2011; Javadian et al., 2014; Sharma et al., 2010]. The process of adsorption compared with other methods comes along to be an attractive process owing to its efficiency, simplicity, ease of operation along with economic feasibility with which it can be implemented in the treatment of heavy metal containing wastewater [Thevannan et al., 2011; Sun et al., 2014; Ozcan and Ozcan, 2013; Kamari et al., 2009].

The objective of this part of study is to explore the adsorption capacity of alumina nanoparticles modified with cetyl trimethyl ammonium bromide (CTAB) for adsorption of Ni(II) from aqueous solutions. The combined effect of initial concentration, pH and adsorbent dose on nickel removal from aqueous solutions has been investigated on Box-Behnken experimental design in response surface methodology (RSM). Besides isotherm and kinetic parameters thermodynamic parameters were also determined for investigation of the feasibility of the adsorption process.

6.2 Results and discussions

6.2.1 Characterization of nano-alumina after adsorption of nickel

The structural and morphological characterization of nano-alumina before adsorption has been discussed in detail in Section 3.2.3 of Chapter 3. After the adsorption of metal ion on the surface, XRD pattern of the adsorbent was compared and absence of any extra peak on the surface revealed that structural changes did not occur during the

process of removal of the metals from aqueous solutions. (Figure 6.1).

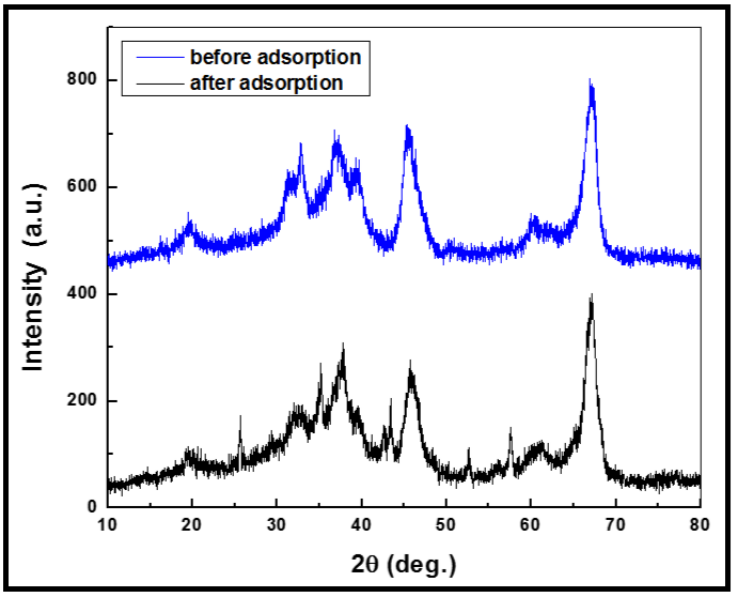

Figure 6.1 XRD pattern of nano-alumina before and after adsorption of Ni(II) ions.

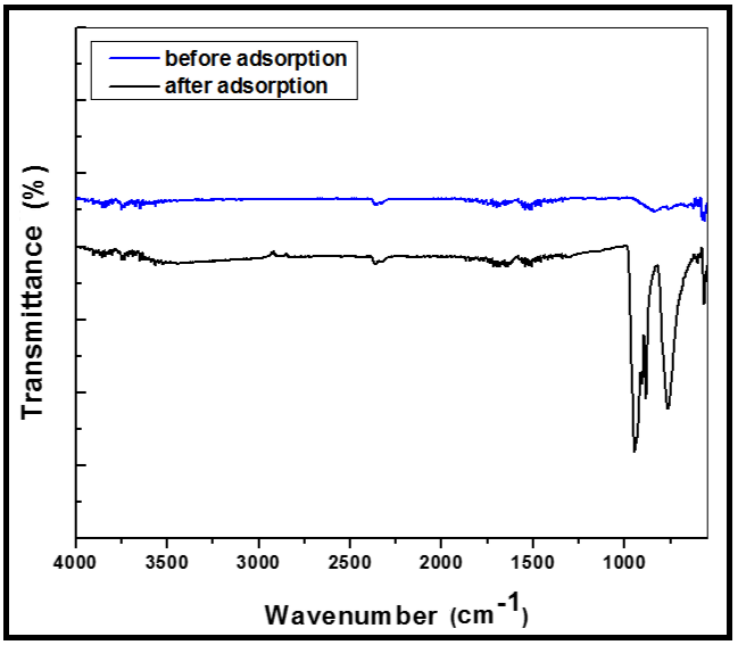

Figure 6.2 FT-IR spectrum of nano-alumina before and after adsorption of Ni(II) ions.

Absence of any extra peak in the material after adsorption evidenced the physical nature of adsorption process (Figure 6.2).

The elemental composition of the material after the adsorption was studied on Energy Dispersive X-ray analysis (EDS) and the presence of peak of Ni in the pattern in addition to the peaks of Al and O evidenced its presence on the surface of the nano-adsorbent (Figure 6.3).

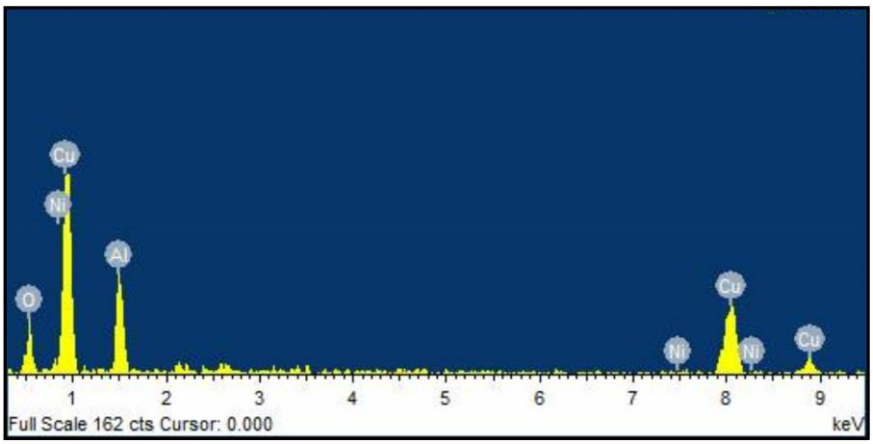

Figure 6.3 EDS pattern of nano-alumina after adsorption.

6.2.2 Adsorption Experiments

The experiments for the removal of Ni from aqueous solutions by adsorption on nano-alumina were carried out in batches. The details of the experiments have been given elsewhere (Section 3.7.1, Chapter 3).

6.2.2.1 Effect of experimental parameters on the removal of nickel from aqueous solution

The preliminary experiments were conducted for investigation of influence of various parameters namely pH, adsorbent dose and initial metal ion concentration and the results exhibited that acidic conditions hindered the adsorption while increasing pH showed increment. The percentage of Ni(II) adsorbed by alumina nanoparticles was increased when the pH of the solution was augmented from 2.0 to 8.0 (Figure 6.4). The optimal removal of Ni in the present system was achieved at pH 7.0, and hence this pH was selected for the rest of the experiments. Similarly, removal percent of nickel was enhanced with increased dosage of adsorbent keeping other experimental conditions incessant as shown in Figure 6.5. The influence of initial metal concentration was investigated by conducting experiments with different initial Ni(II) concentrations ranging from 15 to 40 mg/L. At lower concentration, due to high ratio of available free sites on the adsorbent surface and metal ions in solution the removal percentage is higher for lower concentration and vice versa as shown in Figure 6.6. It was found that removal decreased on raising concentration from 15 mg/L to 40 mg/L. The contact time of the system was evaluated by conducting experiment with 20 mg/L of nickel solution at pH 7.0 and adsorbent dose 10g/L for different time intervals. It was observed that the adsorption rate for metal ion increases in the beginning and after 7 min the adsorption rate become roughly steady and finally adsorption equilibrium was achieved within 7 min (Figure 6.7). After 7 min, there were no significant changes marked in the removal of metal ions.

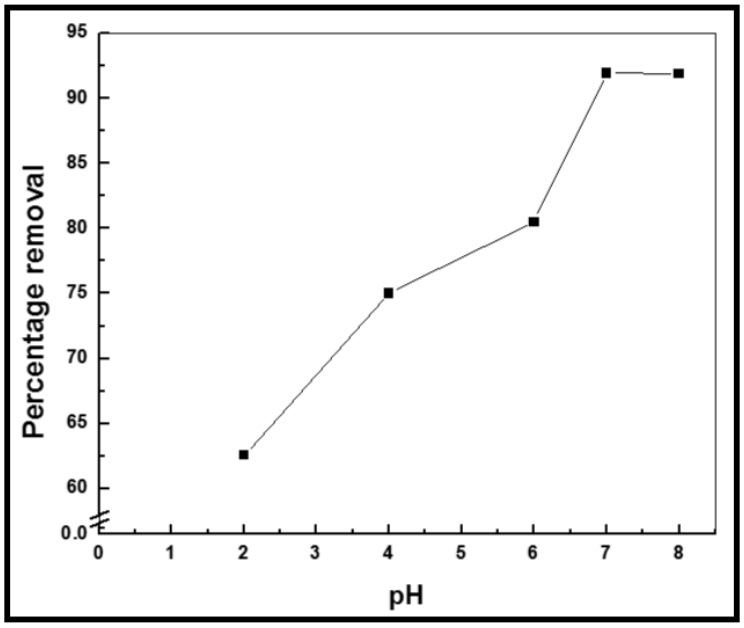

Figure 6.4 Effect of initial pH on removal (%) of nickel from aqueous solution on nano-alumina (Initial concentration= 20 mg/L, adsorbent dose=10 g/L, Temperature= 303K)

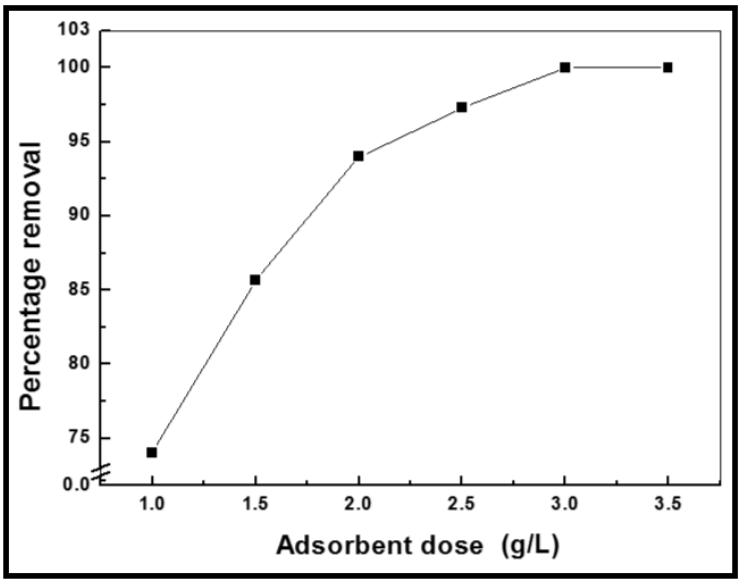

Figure 6.5 Effect of adsorbent dose on removal (%) of nickel from aqueous solution on nano-alumina (Initial pH=7.0, Initial concentration=20mg/L, Temperature 303K)

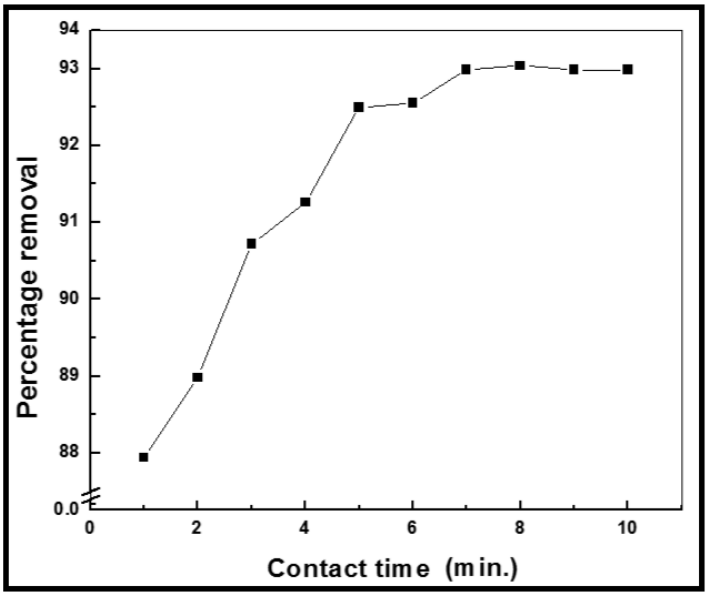

Figure 6.6 Effect of contact time on removal (%) of nickel from aqueous solution on nano-alumina (Initial concentration=20mg/L, Initial pH =7.0, Initial dose=10g/L, Temperature= 303K)

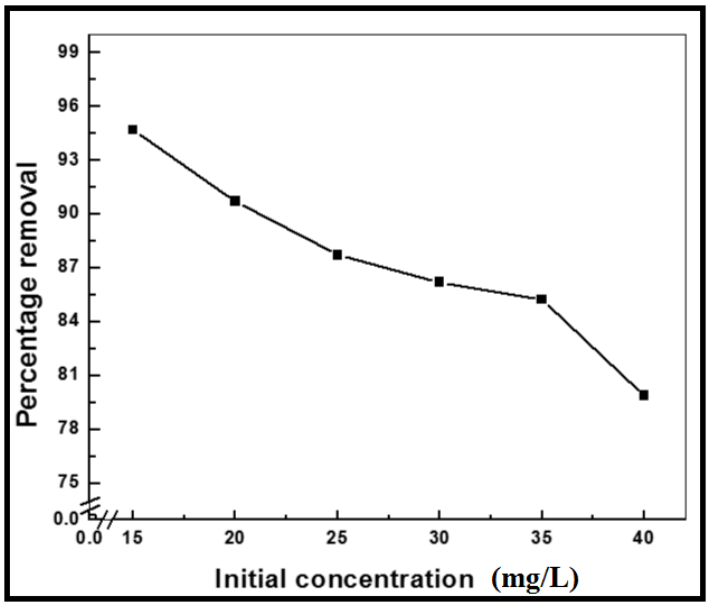

Figure 6.7 Effect of initial concentration on removal (%) of nickel from aqueous solution on nano-alumina (Initial pH= 7.0, Initial dose=10g/L, Temperature=303 K)

6.2.2.2 Design of experiment and data analysis for adsorption of nickel on nano-alumina

The adsorption experiments based on the design matrix of Box-Behnken design of RSM as discussed in Section 3.7.2.2 of Chapter 3 were conducted for obtaining the response corresponding to the independent variables addressed in the experimental design matrix by applying quadratic model and corresponding results obtained has been presented in Table 6.1.

Table 6.1 Box-Behnken designed experimental runs for removal of nickel on nano-alumina

Run Order	Concentration (mg/L)	pH	Dose (g/L)	Percent removal
1	5	2	11	48.31
2	25	2	11	63.24
3	5	7	11	100
4	25	7	11	94.22
5	5	4.5	2	72.87
6	25	4.5	2	67.34
7	5	4.5	20	100
8	25	4.5	20	100
9	15	2	2	54.68
10	15	7	2	71.85
11	15	2	20	55.23
12	15	7	20	100
13	15	4.5	11	99.12
14	15	4.5	11	98.45
15	15	4.5	11	98.55

On the basis of experimental result the empirical relationship between the response and the independent variables, namely initial concentration, pH and adsorbent dose in the coded units is presented in the form of following polynomial regression equation for removal (%) of nickel designated by Y:

$$Y = 98.7067 - 0.4525\,(\text{concentration}) + 18.0762\,(\text{pH}) + 11.0612\,(\text{adsorbent dose}) - 3.8258\,(\text{concentration})^2 - 18.4383\,(\text{pH})^2 - 9.8283\,(\text{adsorbent dose})^2 - 5.1775\,(\text{concentration} \times \text{pH}) + 1.3825\,(\text{concentration} \times \text{adsorbent dose}) - 6.9000\,(\text{pH} \times \text{adsorbent dose}) \quad (6.1)$$

In order to support the hierarchical nature of this model, insignificant terms were still maintained in this study and have been included in the given regression equation [Dahlan et al., 2008]. In the quadratic equation (Equation 6.1) the magnitude of the coefficient portrays the intensity while the sign before the coefficient indicates nature of influence (positive or negative) of the particular variable on the response. A positive sign of a factor means that the response is improved when the factor level augments and a negative effect of the factor revealed that the response is suppressed with the increase in factor level. Upon regression analysis, the regression equation for removal of nickel with alumina nanoparticles yielded regression coefficient $R^2 = 96.42$, higher than the R^2 (adj.) = 89.97. (Table 6.2) that validates the process of adsorption in the given range of experimental conditions.

The parameters bearing positive sign before their corresponding coefficients inclined to increase the nickel removal (%) and vice versa [Sarkar and Majumdar, 2011]. From the equation, it has been deciphered that pH is the most dominating parameter having positive sign before its coefficient followed by adsorbent dose and concentration. Positive sign before coefficients of both pH and concentration suggested the increment in nickel removal (%) with increase in pH and concentration.

Table 6.2 Estimated regression coefficients for removal of nickel on nano-alumina

Term	Coef	SE Coef	T	P
Constant	98.7067	3.667	26.915	0
Concentration	-0.4525	2.246	0.201	0.848
pH	18.0762	2.246	8.049	0
Dose	11.0612	2.246	4.925	0.004
Concentration*Concentration	-3.8258	3.306	-1.157	0.299
pH* pH	-18.4383	3.306	-5.578	0.003
Dose*Dose	-9.8283	3.306	-2.973	0.031
Concentration*pH	-5.1775	3.176	-1.63	0.164
Concentration*Dose	1.3825	3.176	0.435	0.681
pH*Dose	6.9	3.176	2.173	0.082
S = 6.35199 **PRESS = 3224.23**				
R-Sq = 96.42% **R-Sq(pred) = 42.75%** **R-Sq(adj) = 89.97%**				

From the equation (6.1), it has been deciphered that pH is the most dominating parameter having positive sign before its coefficient followed by adsorbent dose and concentration. Positive sign before coefficients of both pH and concentration suggested the increment in nickel removal (%) with increase in pH and concentration.

6.2.2.3 Analysis of variance (ANOVA)

In order to ensure a good model, statistical testing was performed by applying analysis of variance (ANOVA) as discussed in Section 3.7.2.3, Chapter 3 and the results were presented in Table 6.3. In present case, ANOVA study exhibited that the regression model is significant as large F-value and a low P value [Jain et al., 2011]. Among linear effect, pH is the dominant parameter among other having sum of squares (Seq SS) value of 2614.01 followed by adsorbent dose and adsorbent dose. Similarly, among square effect pH*pH was dominant and among interactive effect pH*adsorbent dose was found significant on the basis of sum of squares value.

Table 6.3 Analysis of variance for removal of nickel on nano-alumina

Source	DF	Seq SS	Adj SS	Adj MS	F	P
Regression	9	5429.94	5429.94	603.33	14.95	0.004
Linear	3	3594.45	3594.45	1198.15	29.7	0.001
Concentration	1	1.64	1.64	1.64	0.04	0.848
pH	1	2614.01	2614.01	2614.01	64.79	0
Dose	1	978.81	978.81	978.81	24.26	0.004
Square	3	1530.17	1530.17	510.06	12.64	0.009
Conc*Conc	1	12.19	54.04	54.04	1.34	0.299
pH*pH	1	1161.32	1255.28	1255.28	31.11	0.003
Dose*Dose	1	356.66	356.66	356.66	8.84	0.031
Interaction	3	305.31	305.31	101.77	2.52	0.172
Conc*pH	1	107.23	107.23	107.23	2.66	0.164
Conc*Dose	1	7.65	7.65	7.65	0.19	0.681
pH*Dose	1	190.44	190.44	190.44	4.72	0.082
Residual error	5	201.74	201.74	40.35		
Lack-of-Fit	3	201.48	201.48	67.16	514.11	0.002
Pure Error	2		0.26	0.26	0.13	
Total	14	5631.68				

6.2.2.4 Interaction effect of initial Ni(II) concentration and adsorbent dose

The adsorption experiments based on the matrix predicted by the selected model were conducted with the scheduled concentration range and the desired adsorbent dosage to evaluate their combined effect on the percent removal of nickel ions from the aqueous

solutions. From the regression equation, it is evident that coefficient of concentration is having negative sign that indicates decrease in percent removal with increase in the concentration of solution (Runs "5" and "8'') and (Runs "3" and "10'') This behavior can be attributed to the lesser availability of active sites available on the adsorbent surface due to saturation for interaction with ions present in solution with increase in the concentration of solution [Sharma and Srivastava, 2010, Wang, 2011]. The graphical explication of the interactions of the result of experimentation has been presented in form of contour and surface plots as shown in Figures 6.8a and 6.8b.

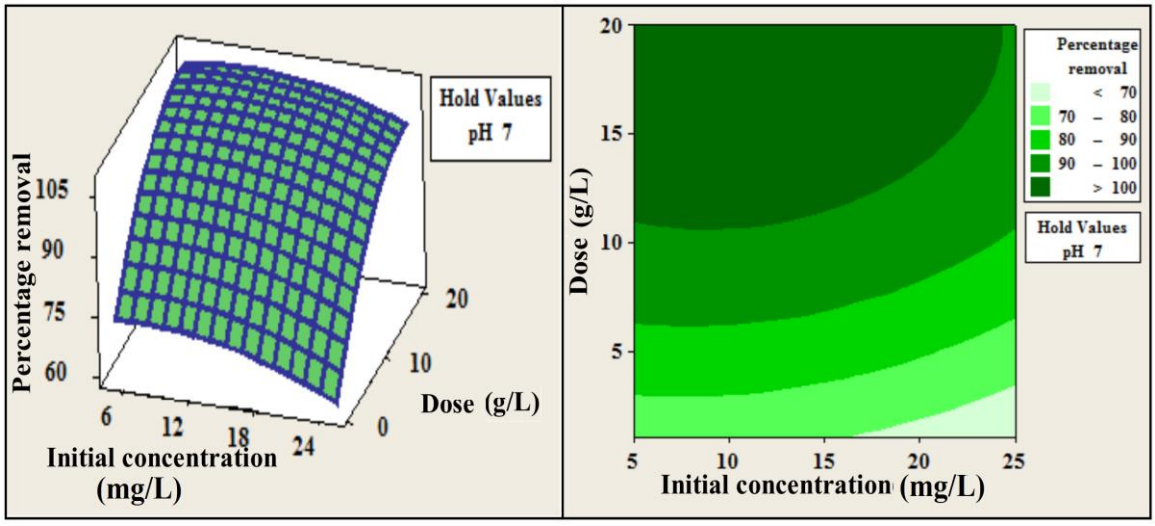

Figure 6.8 (a) Surface plot; and (b) Contour plot of percentage removal vs. dose and concentration at hold value of pH at 7.0

Contour plots and surface plots provide assistance in understanding the relationship between the response and experimental levels of each variable under investigation. Both

these plots revealed that removal percent of Ni(II) decreased on increment in initial metal ion concentration.

6.2.2.5 Interaction effect of pH and adsorbent dose

pH is acknowledged as one of the most important parameter in any adsorption process. It is reported that variation in pH of solution greatly affects the surface of the adsorbent and degree of ionization in solution. Perusal on literature suggested that depending on the pH of the solution, different species of metal ions are present in the solution along with the adsorbate and their removal is greatly influenced by the type of their species present in the system at any particular pH.

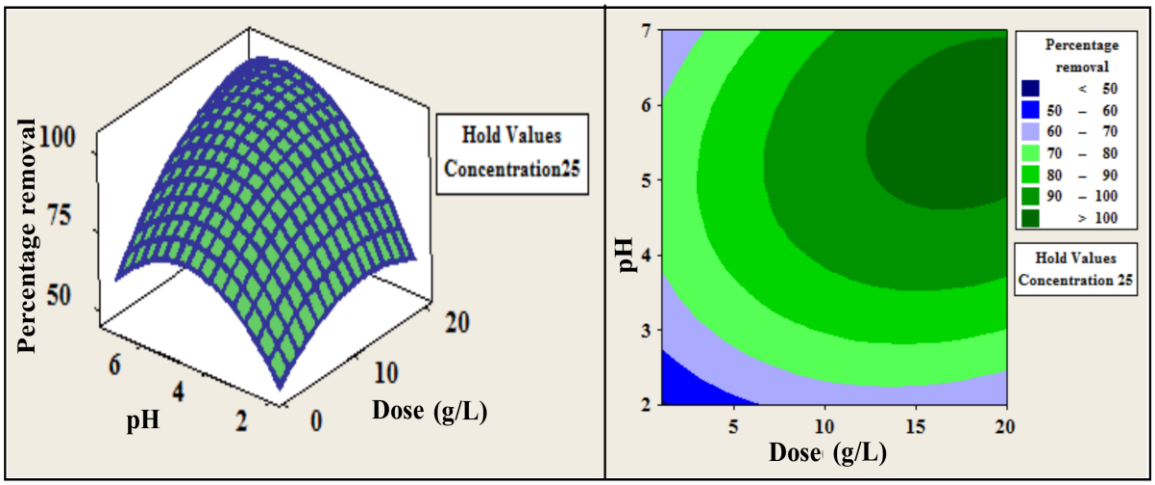

Figure 6.9. (a) Surface plot; and (b) Contour plot of percentage removal vs. pH and dose at hold value of concentration at 25 mg/L

The speciation diagram of Nickel (Figure 3.2, Chapter 3) depicted that Ni^{2+} is the only important oxidation state in its aqueous chemistry up to pH 8.0. The interactive effect of

both these variables viz., pH and adsorbent dose upon adsorption is shown in Figures 6.9a and 6.9b. It has been observed that optimum removal is achieved at higher pH and higher dose, as displayed in (Runs "1" and "5'') and (Runs "4" and "6''). Both these variables collectively depicted that increased number of positive species and surface active sites held responsible for increased percent removal of adsorbate ions [Davarnejad et al., 2015; Reddy et al., 2011].

6.2.2.6 Interaction effect of initial Ni(II) concentration and pH

The adsorption experiments based on the matrix predicted by the selected model were conducted with the scheduled concentration range and the desired adsorbent dosage to evaluate their combined effect on the percent removal of nickel ions from the aqueous solutions. From the regression equation it is evident that coefficient of concentration is having negative sign that indicates decrease in percent removal with increase in the concentration of solution (Runs 1 and 3; Runs 2 and 4). Probably, this behavior can be attributed to the lesser availability of active sites available on the adsorbent surface due to saturation for interaction with ions present in solution with increase in the concentration of solution [Wang, 2011; Sharma and Srivastava, 2010]. The graphical explication of the interactions of the result of experimentation has been presented in the form of contour and surface plots as shown in Figures 6.10a and 6.10b. Both these plots revealed that removal percent of Ni(II) decreased on increment in initial metal ion concentration.

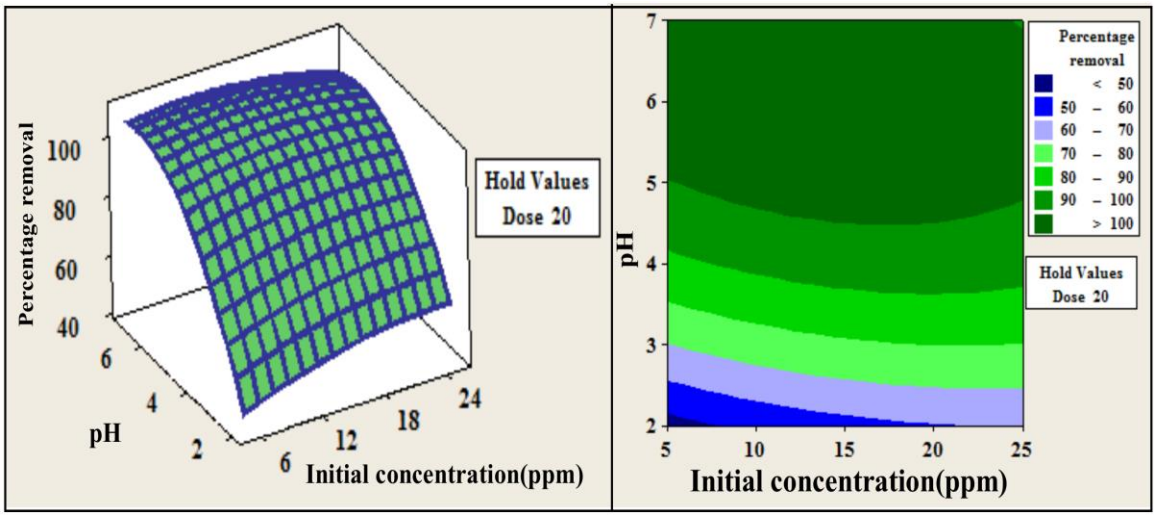

Figure 6.10 (a) Surface plot; and (b) Contour plot of percentage removal vs. pH and concentration at hold value of dose at 20 g/L

6.2.2.7 Interpretation of process optimization of removal (%) of nickel on nano-alumina

The optimum value for desired response was predicted by response optimization plot (Figure 6.11). It predicted the optimum value for 100% removal of Ni(II) from aqueous solutions via the process of adsorption on alumina nanoparticles for the given model (pH 6.89, initial concentration 24.98mg/L, adsorbent dose 19.80 g/L with the desirability score 0.9942. In order to verify the efficacy of model, confirmatory experiments were conducted at the predefined conditions. Further, for the confirmation experiment, pH of the solution, initial concentration and dose were rounded off to 7.0, 25mg/L and 20 g/L, respectively and the experimental results were analyzed.

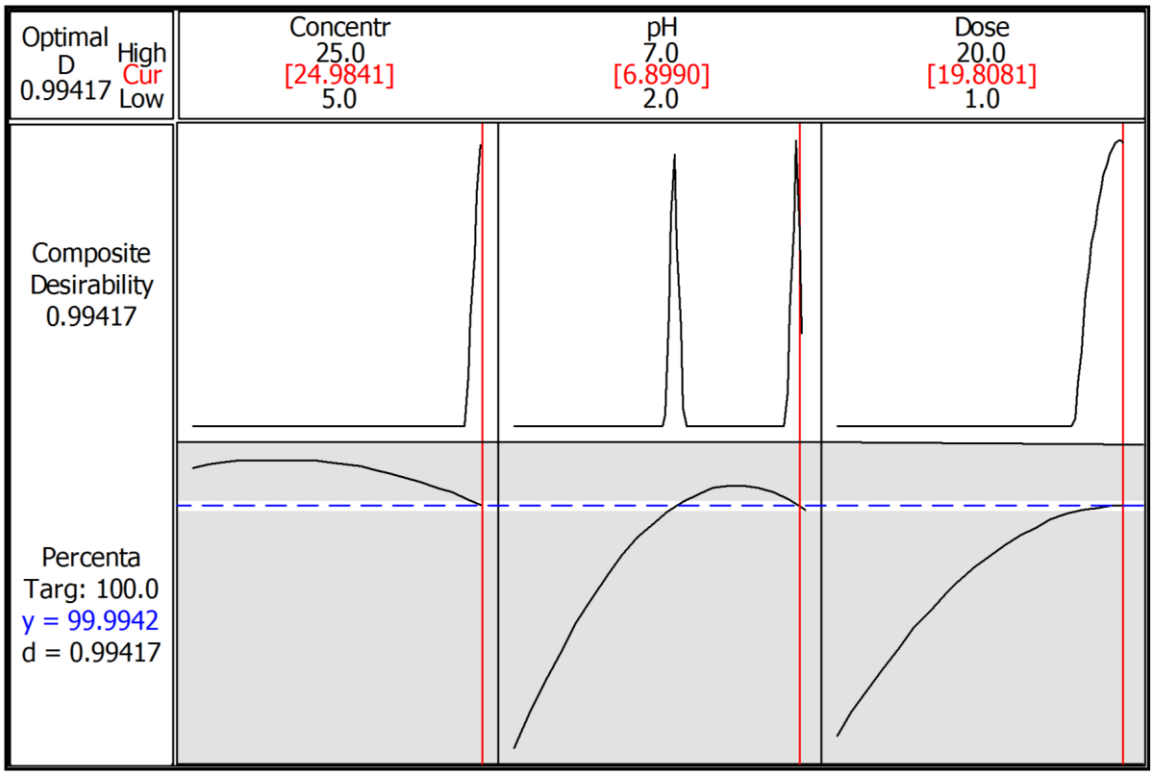

Figure 6.11 Response optimization plot for nickel removal on nano-alumina

However, results showed certain degree of variation than that predicted by the model. The experimental values of the model together with the percentage error difference between the experimental and predicted values have been tabulated in Table 6.4.

Table 6.4 Confirmation experiments for removal of nickel on nano-alumina

S. No.	Concentration (mg/L)	pH	Dose (g/L)	Experimental values (%)	Predicted values (%)
1	20	7	10.0	90.71	92.83
2	25	2	10.0	87.72	87.52
3	20	6	4.0	80.49	82.33
4	25	7	20.0	99.92	100

6.2.3 Adsorption isotherm study

For modelling analysis, operational design and feasibility of the adsorption system, the equilibrium adsorption isotherm furnishes useful information regarding properties and tendency of adsorbent toward adsorbate at given condition at equilibrium [Altin et al. 1998]. In the present study, the equilibrium data incurred for Ni(II) removal was examined with two parameters isotherm viz. Langmuir and Freundlich to ascertain the most desirable one. In addition, linear and non-linear analysis was performed for achieving the best fit isotherm model.

The following linear and non-linear equations of Langmuir isotherm model were used [Langmuir, 1916]:

$$C_e/q_e = 1/bQ^o + C_e/Q^o \quad (6.2)$$

$$q_e = b\,Q^oC_e/1+bC_e \quad (6.3)$$

where, C_e (mg/l) is the equilibrium concentration of the solute, q_e (mg/g) is amount

adsorbed at equilibrium and Q^0 (mg/g) and b (L/mg) are constants related to the adsorption capacity and energy of adsorption, respectively.

Freundlich isotherm model was fitted through following linear and non-linear equations [Freundlich, 1906; Allen and McKay, 1980]:

$$log\ q_e = log\ K_F + 1/n\ log\ C_e \quad (6.4)$$

$$q_e = K_F\ C_e^{1/n} \quad (6.5)$$

where, K_F and n are the Freundlich constants. Here, n giving a sign of how congruous the adsorption process is, and K_F (mg/g(L/mg)$^{1/n}$) represents the quantity of metal ion adsorbed on the adsorbent for a unit equilibrium concentration.

6.2.3.1 Linear analysis of adsorption isotherm

The equilibrium data obtained has been fitted to linear equations of Langmuir and Freundlich adsorption isotherm models to discuss the equilibrium characteristics of the adsorption process. The values of theoretical maximum adsorption capacity, Q^0 (mg g^{-1}) and Langmuir adsorption constant b (L mg^{-1}) were obtained from the slope and intercept of the plot of C_e/q_e vs. C_e, respectively (Figure 6.12) and the parameters of Freundlich isotherm model such as the capacity, K_F (mg g^{-1}) and intensity, n (g L^{-1}) of the adsorption were calculated from the intercept and slope of the linear plot of ln q_e vs. ln C_e, respectively as shown in Figure 6.13. K_F value as well as n showed increment with increase in temperature affirmed the endothermic nature of removal process.

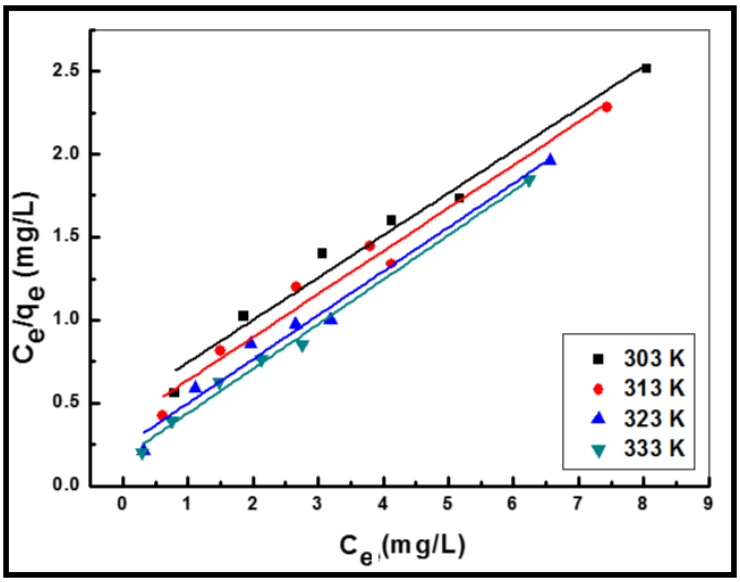

Figure 6.12 Linear Langmuir isotherm plot of nickel removal on nano-alumina (symbols represent the experimental data and straight lines represent the data estimated by the model)

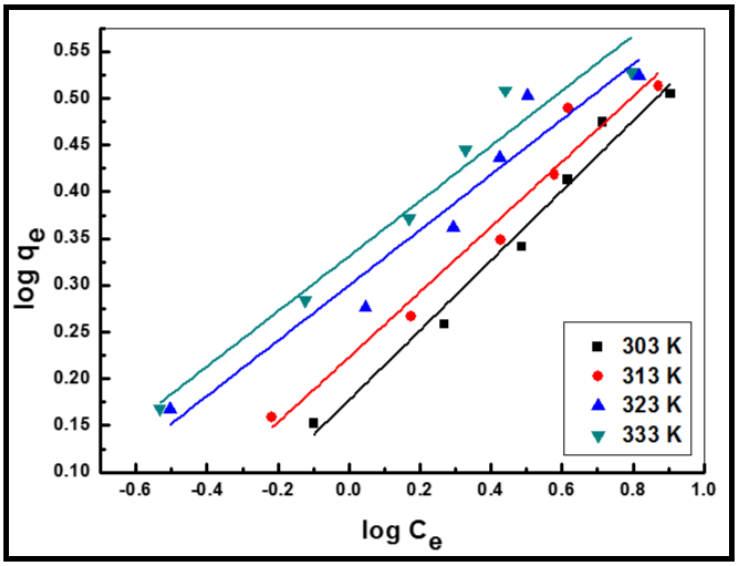

Figure 6.13 Linear Freundlich isotherm plot of nickel removal on nano-alumina (symbols represent the experimental data and straight lines represent the data estimated by the model)

The fitness of experimental data was evaluated at different temperatures and the constant parameters and correlation coefficients (R^2) obtained from the plots of known equation for Langmuir and Freundlich have been summarized in Table 6.5. The high correlation coefficient at all temperatures exhibited that Langmuir model provides the best correlation and thus applicable for interpretation of the experimental data on the whole concentration range.

Table 6.5 Langmuir and Freundlich isotherm parameters for linear analysis and non-linear analysis by Microcal origin for adsorption of nickel from aqueous solution on nano-alumina

Isotherm	**Linear**									
Analysis	**Langmuir Parameters**					**Freundlich Parameters**				
Temperature (K)		**303**	**313**	**323**	**333**		**303**	**313**	**323**	**333**
Constants	**Q^o (mg/g)**	3.72	3.77	3.85	3.92	**K_F (mg/g $(L/mg)^{1/n}$)**	1.50	1.67	1.99	2.14
	b (L/mg)	0.52	0.68	1.13	0.52	**n**	2.68	2.87	3.38	3.39
Coefficient of determination (R^2)		0.99	0.98	0.97	0.97		0.973	0.9548	0.927	0.946

6.2.3.2 Non-linear analysis of adsorption isotherm

Non-linear analysis was performed by altering in-built functions namely Langmuir EXT 1 (Figure 6.14), and Freundlich EXT (Figure 6.15) of origin. In addition to that, user defined isotherm function was used in origin. In user defined equation, initial parameter was taken as numerically one. On curve fitting, both the in-built functions as well as customised user defined functions (Figures 6.16 and 6.17) exhibited difference between the experimental data and data predicted by the models at all the pre-defined temperatures (Table 6.6 and 6.7). Thus, Langmuir isotherm supposed to be the most suitable isotherm model for the present system on the basis of high R^2 adj. value via linear analysis.

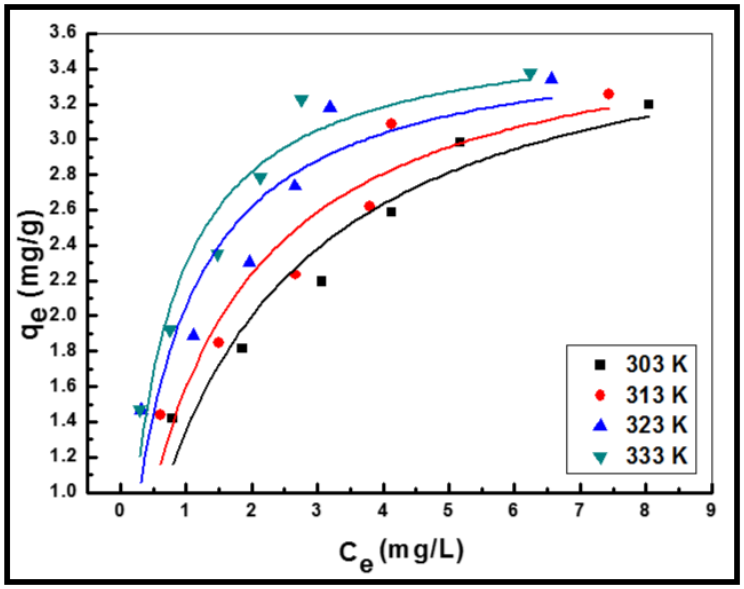

Figure 6.14 Non-linear Langmuir isotherm plot of nickel removal on nano-alumina obtained by in-built Microcal origin function (symbols represent the experimental data and lines represent the data estimated by the model)

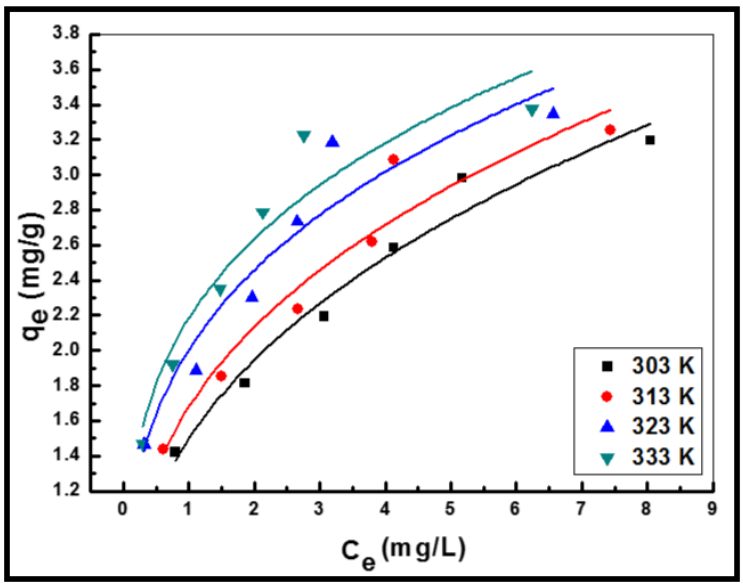

Figure 6.15 Non-linear Freundlich isotherm plot of nickel removal on nano-alumina obtained by in-built Microcal origin function (symbols represent the experimental data and lines represent the data estimated by the model)

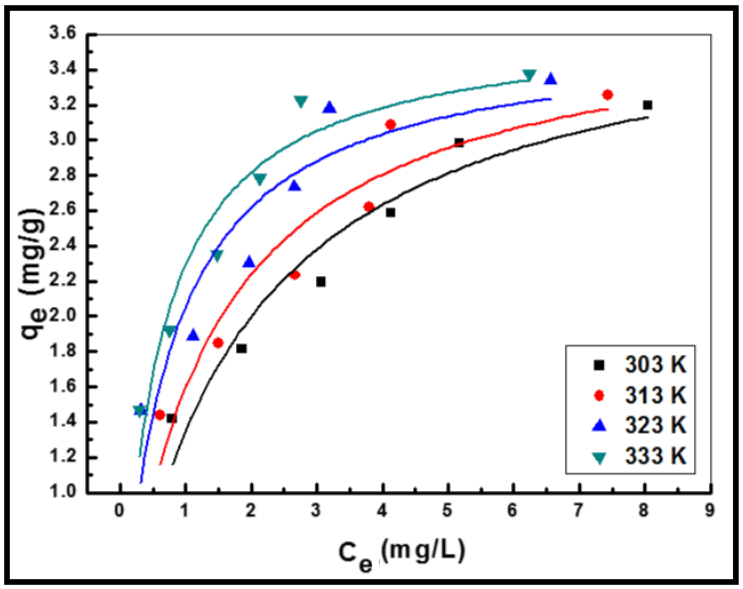

Figure 6.16 Non-linear Langmuir isotherm plot of nickel removal on nano-alumina obtained by customized Microcal origin function (symbols represent the experimental data and lines represent the data estimated by the model)

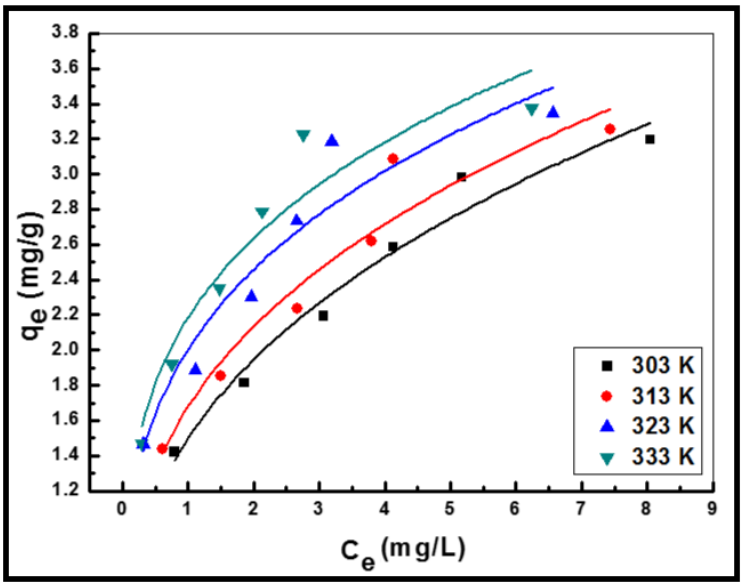

Figure 6.17 Non-linear Freundlich isotherm plot of nickel removal on nano-alumina obtained by customized Microcal origin function (symbols represent the experimental data and lines represent the data estimated by the model)

Table 6.6 Langmuir and Freundlich isotherm parameters for non-linear analysis obtained by in-built Microcal origin functions for adsorption of nickel from aqueous solution on nano-alumina

Analysis	**Non-linear**									
Isotherm	**Langmuir Parameters**					**Freundlich Parameters**				
Temperature (K)		**303**	**313**	**323**	**333**		**303**	**313**	**323**	**333**
Constants	**Q^o (mg/g)**	3.85	3.76	3.61	3.66	**K_F (mg/g $(L/mg)^{1/n}$)**	1.49	1.68	2.00	2.18
	b (L/mg)	0.54	0.74	1.32	1.68	**n**	0.38	0.35	0.29	0.27
Coefficient of determination (R^2)		0.81	0.91	0.87	0.92		0.965	0.923	0.903	0.909

Table 6.7 Langmuir and Freundlich isotherm parameters for non-linear analysis obtained by customized Microcal origin functions for adsorption of nickel from aqueous solution on nano-alumina

Analysis	**Customized**									
Isotherm	**Langmuir Parameters**					**Freundlich Parameters**				
Temperature (K)		**303**	**313**	**323**	**333**		**303**	**313**	**323**	**333**
Constants	**Q^o (mg/g)**	3.85	3.76	3.61	3.66	**K_F (mg/g $(L/mg)^{1/n}$)**	1.49	1.68	2.00	2.18
	b (L/mg)	0.54	0.74	1.32	1.68	**n**	2.65	2.88	3.38	3.68
Coefficient of determination (R^2)		0.81	0.91	0.87	0.92		0.965	0.923	0.903	0.909

6.2.4 Adsorption kinetic modelling

Adsorption process, in general is supposed to be administered by one or more steps (e.g. film diffusion, intra-particle diffusion, and/or pore diffusion). In order to investigate the rate-controlling step, the mechanism of interaction of adsorbent and adsorbate, rate of uptake of metallic species as contaminant the adsorption data has been fitted to kinetic models, namely pseudo-first-order, pseudo-second-order and intra-particle diffusion models [Uma et al. 2013]. Meanwhile, linear and non-linear analysis of the adsorption data has been carried out in order to achieve the best fit kinetic model.

The pseudo-first-order kinetic model has been widely used to predict the sorption kinetics and can be expressed by the following linear and non-linear equations [Hodaifa et al., 2013]:

$$dq/dt = k_1 (q_e - q_t) \quad (6.6)$$

$$ln (q_e - q_t) = ln\, q_e - k_1 t \quad (6.7)$$

$$q_t = q_e (1 - exp (-k_1 t)) \quad (6.8)$$

where, k_1(min^{-1}) is the first order rate constant, q_e and q_t are the amount of adsorbate species adsorbed on adsorbent at equilibrium and at any time, t, respectively.

Pseudo-second order model is based on the assumption that the rate limiting step is chemi-sorption in nature. The model is represented in the form of following linear and non-linear equations [Ho and McKay, 1998]:

$$dq/dt = k_2 (q_e - q_t)^2 \quad (6.9)$$

$$q_t = k_2 q_e^2\, t / 1 + k_2\, q_e\, t \quad (6.10)$$

where, k_2(g mg^{-1} min^{-1}) is the rate constant for pseudo-second-order model equation.

6.2.4.1 Linear analysis of adsorption kinetics

During linear analysis, for the pseudo-first-order model (Lagergren model), the kinetic parameters viz., k_1 and q_e values was determined from the slope and intercept of the plot of log (q_e-q_t) vs. t, respectively (Figure 6.18). Likewise, the plot of t/q_t vs. t for

the pseudo-second-order kinetic model yielded a straight line from which k_2 and the equilibrium adsorption capacity (q_e) were calculated from the intercept and slope of this line, respectively as shown in Figure 6.19.

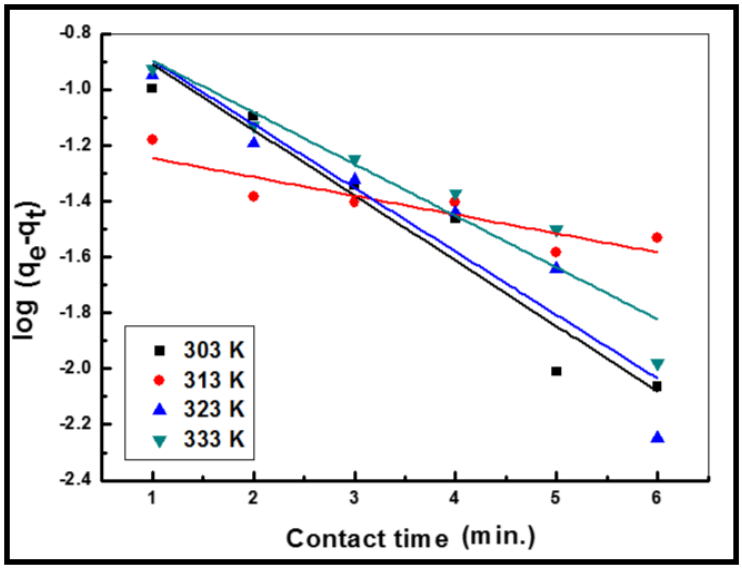

Figure 6.18 Linear pseudo-first order plot of nickel removal on nano-alumina (symbols represent the experimental data and straight lines represent the data estimated by the model)

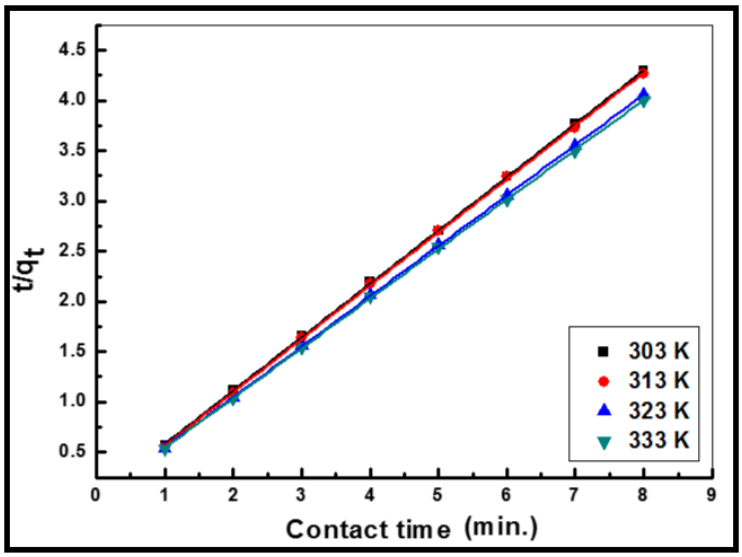

Figure 6.19 Linear pseudo-second order plot of nickel removal on nano-alumina (symbols represent the experimental data and straight lines represent the data estimated by the model)

The values of different parameters as determined from the pseudo-first-order and pseudo-second-order kinetic model along with their corresponding correlation coefficients were presented in Table 6.8.

It was found that q_e(cal) values from pseudo-first-order model were not reasonably close to experimental q_e(exp) values which showed that the system did not followed pseudo-first-order model. In pseudo-second-order kinetic model, the values of q_e(cal) were very close to q_e(exp) values for all temperatures under study. The value of correlation coefficient (R^2) for pseudo-first-order model was lower as compared to pseudo-second-order kinetics model. Thus, it was inferred from the value of R^2 and closeness of experimental and theoretical adsorption capacity (q_e) that pseudo-second order kinetic model better explained the experimental data on linear analysis.

Table 6.8 Pseudo-first order and pseudo-second order kinetic parameters for linear analysis and non-linear analysis by Microcal origin for adsorption of nickel from aqueous solution on nano-alumina

Kinetic model	**Pseudo-first order Parameter**						
Analysis		**Linear**			**Non-linear**		
Temperature (K)	**q_e (exp.)**	**q_e (mg/g)**	**k_1 (1/min)**	**R^2 adj.**	**q_e (mg/g)**	**k_1 (1/min)**	**R^2 adj.**
303	1.859	0.211	0.54	0.927	1.831	3.17	0.428
313	1.878	0.066	0.16	0.759	1.848	3.89	0.396
323	1.971	0.215	0.53	0.875	1.943	3.09	0.627
333	1.999	0.195	0.43	0.899	1.965	3.12	0.551
Kinetic model	**Pseudo-second order Parameter**						
Analysis		**Linear**			**Non-linear**		
Temperature (K)	**q_e (exp.)**	**q_e (mg/g)**	**k_2 (g.mg^{-1} min^{-1})**	**R^2 adj.**	**q_e (mg/g)**	**k_2 (g.mg^{-1} min^{-1})**	**R^2 adj.**
303	1.859	1.884	5.19	0.999	1.865	14.56	0.838
313	1.878	1.887	7.39	0.999	1.864	32.55	0.645
323	1.971	1.994	5.22	0.999	1.978	14.73	0.928
333	1.999	2.024	4.57	0.999	2.001	14.65	0.886

6.2.4.2 Non-linear analysis of adsorption kinetics

For non-linear analysis of adsorption data curve fitting was done by altering in built functions of Microcal origin namely Langmuir EXT 1 and BoxLucas 1 to coincide with pseudo-first order (Figure 6.20) and pseudo-second order (Figure 6.21) kinetics equations respectively. Customized user defined isotherm function was also used in which initial parameter was taken as numerically one similar to that of the non-linear analysis of isotherm (Figures 6.22 and 6.23). The experimental data and data estimated by both the in-built and customized Microcal origin functions showed a vast difference on non-linear analysis. Thus, on the basis of high R^2 adj. values, linear approach for determination of kinetic parameter was preferred over non-linear analysis.

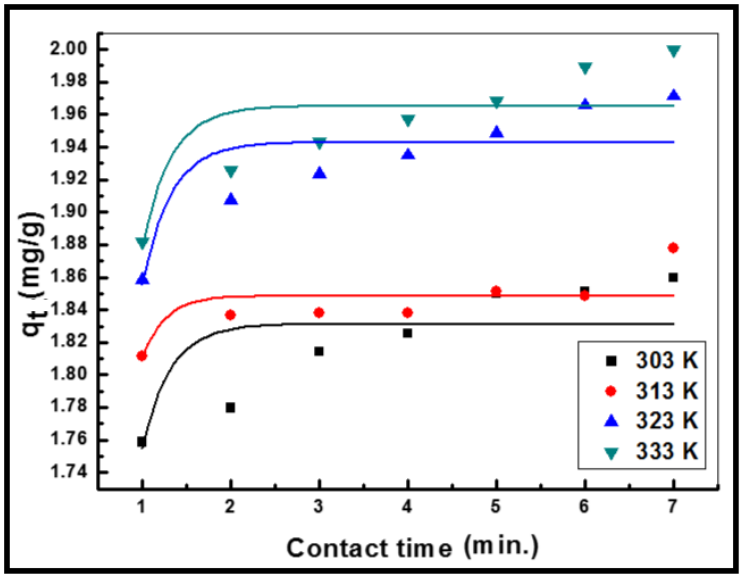

Figure 6.20 Non-linear pseudo-first order plot of nickel removal on nano- alumina obtained by in-built Microcal origin function (symbols represent the experimental data and lines represent the data estimated by the model)

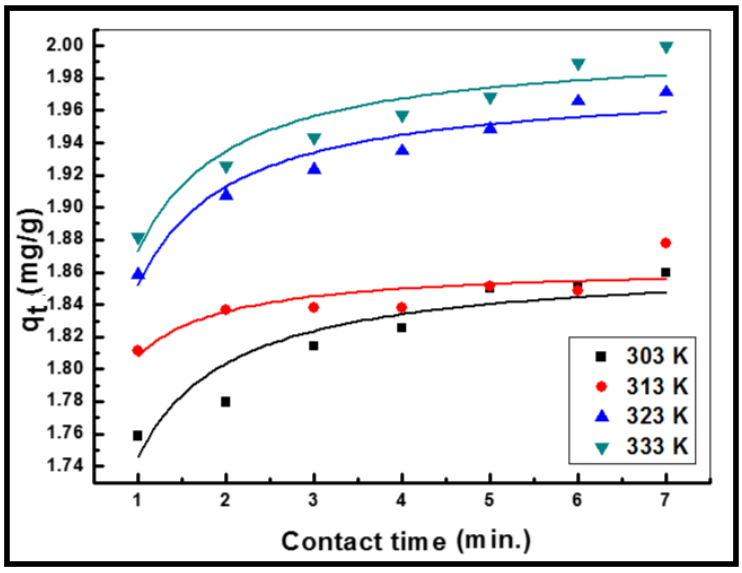

Figure 6.21 Non-linear pseudo-second order plot of nickel removal on nano- alumina obtained by in-built Microcal origin function (symbols represent the experimental data and lines represent the data estimated by the model)

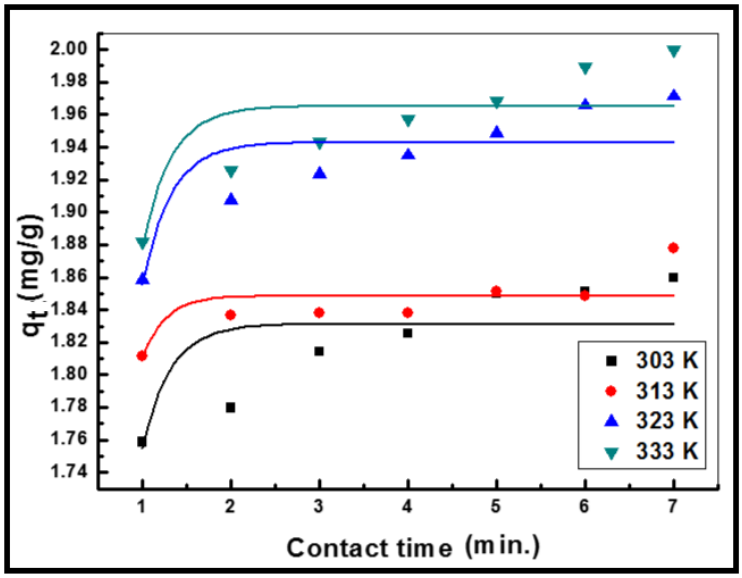

Figure 6.22 Non-linear pseudo-first order plot of nickel removal on nano-alumina obtained by customized Microcal origin function (symbols represent the experimental data and lines represent the data estimated by the model)

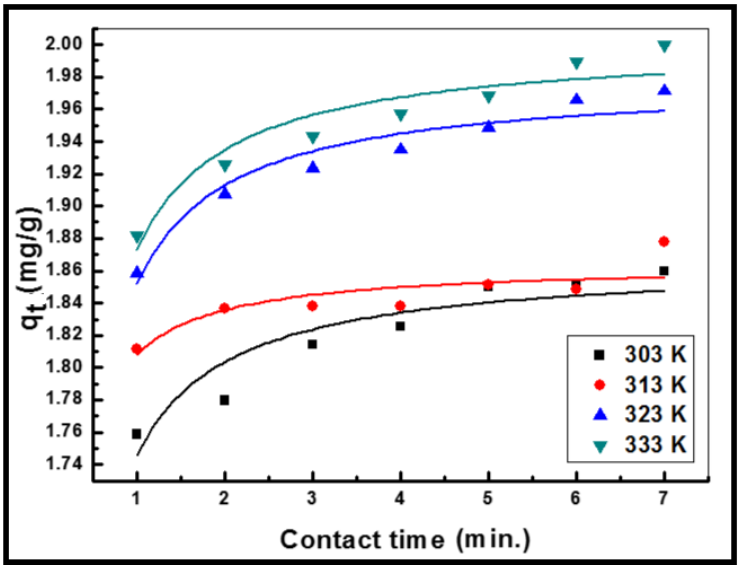

Figure 6.23 Non-linear pseudo-second order plot of nickel removal on nano-alumina obtained by customized Microcal origin function (symbols represent the experimental data and lines represent the data estimated by the model)

Table 6.9 Pseudo-first order and pseudo-second order kinetic parameters for linear analysis and non-linear analysis by customized Microcal origin for adsorption of nickel from aqueous solution on nano-alumina

Analysis	**Customized**						
Kinetic model		**Pseudo-first order Parameter**			**Pseudo-second order Parameter**		
Temperature (K)	**q_e (exp.)**	**q_e (mg/g)**	**k_1 (1/min)**	**R^2 adj.**	**q_e (mg/g)**	**k_1 (1/min)**	**R^2 adj.**
303	1.859	1.831	3.17	0.428	7.803	1.86	0.838
313	1.878	1.848	3.89	0.397	17.46	1.86	0.645
323	1.971	1.943	3.09	0.627	7.449	1.98	0.928
333	1.999	1.965	3.12	0.551	7.322	2.00	0.886

6.2.4.3 Intra-particle diffusion

Later on, the process possibility was explored on the intra-particle diffusion model based on diffusive mass transfer where the adsorption rate expressed in terms of the square root of time (t) [Weber and Morris, 1963]:

$$q_t = K_{id}\, t^{0.5} + C \qquad (6.11)$$

The plot of q_t vs. the square root of time at different temperatures has been shown in Figure 6.24A. The values of intra-particle diffusion rate constant, K_{id} (mg $g^{-1}min^{-1/2}$) and film thickness, C (mg g^{-1}) calculated from the intercept and slope of the plot, respectively along with their correlation coefficients has been presented in Table 6.10.

The intra-particle diffusion plot has been demarcated into three regions being marked as 1, 2 and 3 where each domain has its own significance. The regions 1 and 2 represent

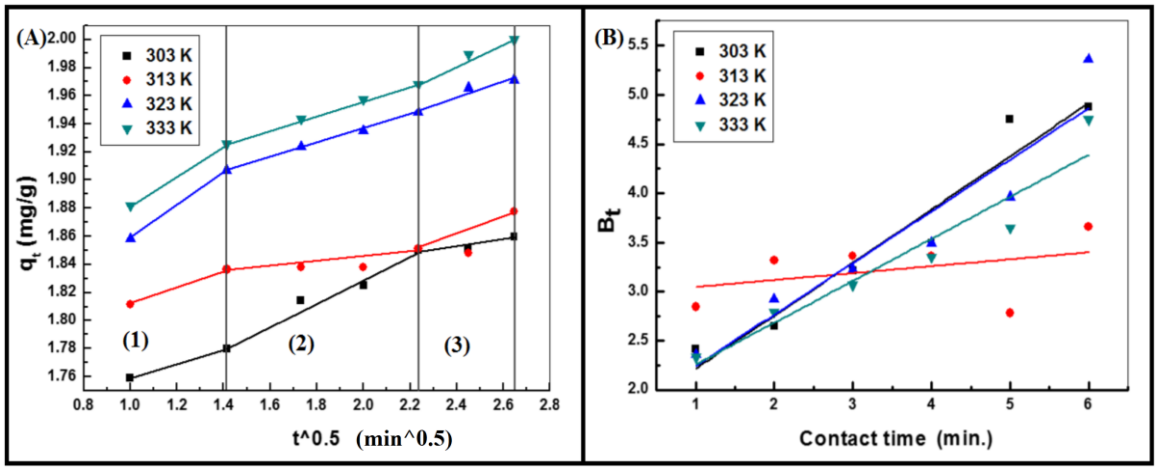

Figure 6.24 A) Intra-particle diffusion plot for removal of nickel from aqueous solution on nano-alumina. B) Boyd model plot for removal of nickel from aqueous solution on nano-alumina

film diffusion and intra-particle diffusion respectively, whereas region 3 represented the interior surface of adsorbent where adsorption occurred. The probability of intra-particle diffusion to be the rate-controlling step in the process has been ascertained by the plot that must pass through the origin (C=0), but it was noticed that plots didn't pass through the origin. However, high determination coefficient suggested significant role of intra-particle diffusion in the initial stages of adsorption process but was not the rate-governing step [Mohanty et al., 2005; Stankovic´ et al., 2016].

Table 6.10 Intra-particle diffusion constant values for removal of nickel from aqueous solution on nano-alumina

S. No.	Concentration (mg/L)	K_{id} (mg/g $min^{1/2}$)	C (mg/g)	R^2
1	303	0.065	1.69	0.965
2	313	0.031	1.78	0.789
3	323	0.065	1.80	0.959
4	333	0.068	1.82	0.979

6.4.2 Boyd model

In order to explore the probable mechanism of adsorption further, the Boyd model was applied on the kinetic data. This model distinguishes the film diffusion (boundary

layer) and pore diffusion (diffusion inside adsorbent pores). It can be expressed in the following form [Hu, et al., 2011]:

$$B_t = -0.4977 - ln\ (1 - F) \quad (6.12)$$

where, F is the fraction of adsorbed adsorbate at any time t (min). Bt was plotted against t and in the present case, the line (Figure 6.24 B) did not pass through origin. It indicated that adsorption has been governed by boundary layer diffusion mechanism.

6.2.5 Adsorption thermodynamic study

6.2.5.1 Effect of temperature

The influence of temperature on the removal of Ni(II) has been investigated at different temperature ranges from 303 to 333 K and at various concentrations pre-defined for the experimentation. It was ascertained that percent removal get augmented with the temperature which may be due to the increase in number of active sites on the surface of adsorbent and this trend suggests the endothermic nature of the adsorption process (Figure 6.25) [Chen et al., 2011].

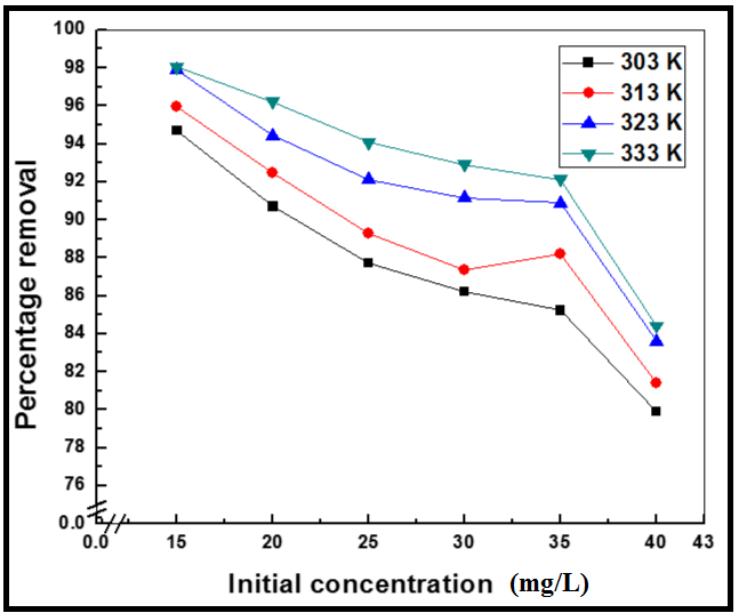

Figure 6.25 Effect of temperature on removal of nickel from aqueous solutions on nano-alumina

6.2.5.2 Thermodynamic parameters

Thermodynamic parameters such as changes in standard free energy (ΔG˚), enthalpy (ΔH˚), and entropy (ΔS˚) were evaluated from Langmuir adsorption model to confirm the adsorption nature of the present study. The following equations have been used for their estimation [Salvestrini et al., 2014; Brown et al., 2009; Elkady et al., 2011]:

$$\Delta G^{\circ} = - RT \ln K_L \quad (6.13)$$

$$\ln K_L = \Delta S^{\circ}/R - \Delta H^{\circ}/RT \quad (6.14)$$

where, ΔG° is the Gibbs free energy change, Langmuir constant b is considered as thermodynamic equilibrium constant; K_L (L mol^{-1}), R is universal gas constant (8.314

J•mol^{-1}•K^{-1}), and T is the absolute temperature in Kelvin. Subsequently, the values of ΔHº and ΔSº were also determined from the slope and intercept of the plot of ln K_L vs. 1/T, respectively. The values of ΔG°, ΔH° and ΔS° calculated at different temperatures have been tabulated in Table 6.11.

The negative ΔG◦ values affirm the feasibility of the adsorption process as well as the spontaneous nature of adsorption that do not require any external source of energy for its occurrence. Further, the increase in negative value at higher temperature suggested that the spontaneity of adsorption process increased with rise in temperature. In case of physi-sorption the change of standard free energy varies in the range of −20 to 0 kJ mol^{-1} while for involvement of chemi-sorption standard free energy varies in the range −80 and −400 kJ mol^{-1} (Avila et al. 2014).

Table 6.11 Thermodynamic parameters for adsorption of nickel from aqueous solution on nano-alumina

S. No.	Temperature (K)	Δ G◦ (kJ mol^{-1})	ΔH◦ (kJ mol^{-1})	ΔS◦ (J mol^{-1}K^{-1})
1	303	-25.99	32.13	190.5
2	313	-27.57		
3	323	-29.80		
4	333	-31.65		

Furthermore, the (ΔH◦) values were also found to be very low and positive (32.13 kJ mol^{-1}) which indicated the physi-sorption of Ni(II) on alumina nanoparticles which was also evident from various characterizations after adsorption besides exhibiting endothermic nature [Sharma et al. 2010]. The positive value 190.5 J $mol^{-1}K^{-1}$ of entropy (ΔS◦) suggested good affinity of Ni(II) towards the nanoparticles and showed increased randomness at the solid/solution interface during the adsorption process.

6.2.5.3 Activation energy

Activation energy is defined as the energy that must be overcome in order for a chemical reaction to occur. Being specific to adsorption processes, it is defined as the minimum energy needed for a specific adsorbate-adsorbent interaction to take place, despite the fact that the process may be thermodynamically feasible The activation energy (E_a) for the adsorption of an adsorbate ion/molecule onto an adsorbent surface in an adsorption process can be evaluated from the Arrhenius equation as follows [Aksu, 2002]:

$$ln\ k_2 = ln\ A - E_a/RT \qquad (6.15)$$

where, k_2 (g mg^{-1} min^{-1}) represents the rate constant obtained from the pseudo-second order kinetic model, E_a (J mol^{-1}) is the Arrhenius activation energy of adsorption and A is the Arrhenius factor. The values of E_a and A can be obtained from the slope and the

intercept from the plot of ln k_2 versus 1/T (Figure 6.26). The activation energy was estimated as -5.87 kJ mol^{-1}.

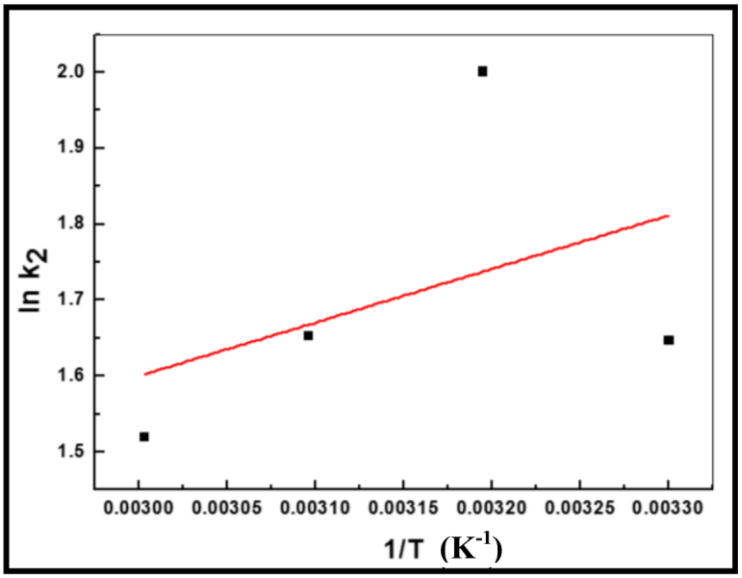

Figure 6.26 Arrhenius plot for removal of nickel from aqueous solution on nano-alumina

6.6 Desorption experiments

The possibility of reuse of exhausted adsorbent has been substantiated by conducting desorption experiments with three desorbing agents namely HCl (Hydrochloric acid), HNO_3 (Nitric acid) and H_2SO_4 (Sulfuric acid). 0.1N of the aforesaid solutions were prepared and used to desorb the adsorbed nickel ions from the adsorbent and have shown desorption efficiencies of the order of 79.85 %, 89.51 % and 98.68 % respectively.

Among all the solutions maximum desorption efficiency has been exhibited by H_2SO_4 solution and thus it was selected for the desorption purpose. It was found that up to three cycles adsorbent exhibited considerable removal of nickel for reuse as an adsorbent after third cycle the desorption efficiency was reduced (Table 6.12).

Table 6.12 Nickel removal after subsequent regeneration cycle (Initial conc. =20 mg/L pH = 7.0, Dose = 10 g/L, Temperature =303 K)

S. No.	Regeneration cycle	Nickel removal (%)
1	1	98.95
2	2	96.45
3	3	92.37
4	4	79.93

6.7 Conclusions

Ni(II) adsorption on γ-alumina nano-adsorbent was investigated and conditions were optimized on RSM techniques under BBD statistical design. Among various operational parameters such as pH, adsorbent dose and initial concentration, pH of solution has pronounced effect on removal followed by adsorbent dose and initial

concentration. Equilibrium time was found 7 min for adsorption. The adsorptive removal of Ni(II) was endothermic, feasible and spontaneous in nature. Under the conditions predicted by the model, the optimum result can be achieved at pH 7.0, initial concentration 25mg/L and adsorbent dose 20 g/L. Linear approach of kinetic and isotherm determination best explained the data. Pseudo-second-order kinetic and Langmuir isotherm models best fitted to the adsorption data. The experimental results depicted that under optimized conditions, γ-alumina can be used as a potential candidate for treatment of industrial effluents containing nickel ions.